

Adducts of Zirconium and Hafnium Tetrachlorides with Neutral Lewis Bases Part I. Structure and Stability: a Vibrational and NMR Study

MARIANNE TURIN-ROSSIER*, DEIRDRE HUGI-CLEARY and ANDRÉ E. MERBACH**

Institut de Chimie Minérale et Analytique, Université de Lausanne, 3, Place du Château, CH-1005 Lausanne (Switzerland)

(Received June 8, 1989; revised September 12, 1989)

Abstract

Raman and NMR spectroscopy were used to establish the structure and stability of several $MCl_4 \cdot 2L$ adducts ($M = Zr, Hf$; $L =$ neutral Lewis base) in $CHCl_3$ and CH_2Cl_2 . Only *trans* adducts were found for $MCl_4 \cdot 2(Me_2N)_3PO$, *cis-trans* equilibria were observed for $HfCl_4 \cdot 2Cl_2(Me_2N)PO$, $MCl_4 \cdot 2Cl_2(Me_2N)_2PO$ and $MCl_4 \cdot 2(MeO)_3PO$ and only the *cis* configuration was present for $ZrCl_4 \cdot 2Cl_2(Me_2N)PO$, $MCl_4 \cdot 2Cl_2(MeO)PO$ and $MCl_4 \cdot 2L$ ($L = Me_2O, Me_2S, Me_2Se, Cl_3PO$). 1H NMR was used to determine the relative stabilities of some of the adducts and the sequence found was: $(Me_2N)_3PO \gg Cl(Me_2N)_2PO > (MeO)_3PO \gg Cl(MeO)_2PO > Cl_2(Me_2N)PO$. The observed structures and stabilities are explained using steric and electronic arguments. A variable pressure study of the *cis-trans* equilibrium on $ZrCl_4 \cdot 2(MeO)_3PO$ yielded the reaction volume, $\Delta V^\circ = +3.8 \pm 0.4 \text{ cm}^3 \text{ mol}^{-1}$.

Introduction

In order to rationalize the understanding of the mechanisms of substitution and isomerization of octahedral complexes with high oxidation state centres we have undertaken a comprehensive structural and dynamic investigation of the adducts formed between d^0 and d^{10} metal halides and neutral Lewis bases. Studies have been completed for $MX_5 \cdot L$ ($M = Nb, Ta$ [1–4], Sb [5, 6] and $MX_4 \cdot 2L$ ($M = Sn$ [7–11], Ti [12, 13]) adducts. The study of intermolecular exchange reactions between free and coordinated L in inert diluent, and of the *cis-trans* isomerization process on the $MX_4 \cdot 2L$ species is particularly attractive because they occur in single steps, making mechanistic assignment much easier.

We are now extending our investigation to the $Zr(IV)$ and $Hf(IV)$ tetrachloride adducts. In this paper we use vibrational spectroscopy to identify *cis* and/or *trans* isomers. NMR spectroscopy, which does

not provide structural *cis/trans* assignment, is used to complement the vibrational results by supplying quantitative information about the isomerization constants. The relative stability constants of adducts of a metal tetrachloride with different ligands can also be determined from the observation of competitive equilibria. This structural and stability study will lay the foundations for the NMR dynamic analysis reported in a following paper.

Experimental

Sample Preparation

$ZrCl_4$, $HfCl_4$ and their adducts are prone to hydrolysis from atmospheric water, thus all sample manipulation was carried out in a dry glove box (less than 2 ppm water). $ZrCl_4$ (Merck, puriss 99.9%) and $HfCl_4$ (ROC/RIC, puriss 99.9% and Merck, puriss 99.9%) were used without further purification. Chloroform was purified by passing it through a column containing basic Al_2O_3 , and then stored over molecular sieves. The various solvents and Lewis base ligands were prepared and dried using standard methods and were stored over molecular sieves.

Sample solutions were prepared by mixing appropriate quantities of the metal halide, the solvent and the ligand. For the vibrational studies $CHBr_3$, CH_2Br_2 and a 1:3 $CH_2Br_2:CH_3NO_2$ mixture were used as solvents. The [metal chloride]: [total ligand] ratio varied from 1:4 to 1:8 depending on the solubility of the metal adducts. The metal halide concentration varied between 0.1 and 0.3 m (mol kg^{-1} solvent). For the NMR measurements mixtures of normal and deuterated CH_2Cl_2 or $CHCl_3$ were chosen as solvents. The metal halide concentration ranged from 0.01 and 0.1 m and the [metal chloride]: [total ligand] ratio was between 1:3 and 1:4.

Vibrational Spectroscopy

Raman spectra were recorded between 500 and 100 cm^{-1} on a SPEX 1403 spectrometer, using the 514 nm line of an argon laser. The instrument was calibrated using the 218 cm^{-1} band of CCl_4 and the samples were contained in glass capillary tubes.

*Taken, in part, from the Ph.D. Thesis of M.T.

**Author to whom correspondence should be addressed.

NMR Spectroscopy

Ambient pressure proton NMR spectra were recorded at 60 MHz using a Bruker WP-60 spectrometer and at 400 MHz using a Bruker WH-400 spectrometer. At 60 MHz 20 to 100 scans of 4096 points were accumulated over a sweepwidth of 720 Hz, and at 400 MHz 10 to 20 scans of 8192 points were accumulated using a sweepwidth of 2100 Hz. In both cases the field was locked on the deuterium signal of the solvent. $^{31}\text{P}\{^1\text{H}\}$ spectra were obtained at 36.43 MHz on a Bruker HX-90 spectrometer. The temperature was measured by a substitution technique using a platinum resistor [14]. Variable pressure proton measurements were made at 400 MHz on a Bruker AM-400 spectrometer using a home built probe with a deuterium field lock [15] and the temperature was measured using a platinum resistor [16].

For the proton measurements all chemical shifts were referenced to TMS and the ^{31}P chemical shifts were referenced to 62.5% H_3PO_4 . The high frequency convention is used throughout.

Results

Vibrational Spectroscopy

If the ligands are treated as point masses, the symmetry group of *cis*- $\text{MCl}_4 \cdot 2\text{L}$ ($\text{M} = \text{Zr}, \text{Hf}$) is C_{2v} and that of *trans*- $\text{MCl}_4 \cdot 2\text{L}$ is D_{4h} . The vibrational representation for C_{2v} symmetry is $\Gamma_{C_{2v}} = 6A_1 + 2A_2 + 3B_1 + 4B_2$, of which the $A_1 + B_2$ modes represent the M-L bond stretches and the $2A_1 + B_1 + B_2$ modes represent the M-Cl stretches. The A_1 , B_1 , and B_2 vibrational modes are Raman and IR active. In the case of D_{4h} symmetry, the vibrational representation is $\Gamma_{D_{4h}} = 2A_{1g} + B_{1g} + B_{2g} + E_g + 2A_{2u} + 3E_u + B_{2u}$, of which the M-L bond stretches correspond to $A_{1g} + A_{2u}$, while the M-Cl stretches correspond to $A_{1g} + B_{1g} + E_u$. The A_{1g} , and B_{1g} modes are Raman active and the A_{2u} and E_u vibrational modes are IR active.

Solution Raman spectra were taken of a selection of $\text{MCl}_4 \cdot 2\text{L}$ ($\text{M} = \text{Zr}, \text{Hf}$) adducts (see Table 1). The frequencies for the metal chloride stretching vibrations were assigned using Beattie's results for a normal coordinate analysis of *cis*- and *trans*- $\text{MX}_4 \cdot 2\text{L}$ species [17], taking into account the mutual exclusion rule for the *trans* isomer and the fact that the symmetric vibrations will be polarized in solution. Those adducts showing two polarized bands exist only in the *cis* configuration, i.e. $\text{L} = \text{Me}_2\text{O}, \text{Me}_2\text{S}$ and Me_2Se . For $\text{ZrCl}_4 \cdot 2(\text{MeO})_3\text{PO}$ and $\text{HfCl}_4 \cdot 2(\text{MeO})_3\text{PO}$ three polarized bands were observed so both *cis* and *trans* isomers are presumed to occur in these solutions. In order to assign the different bands the lower symmetry of the *cis* isomer is brought into play. This isomer possesses a dipole moment, and

TABLE 1. M-Cl ($\text{M} = \text{Zr}, \text{Hf}$) Raman vibrational stretching frequencies (cm^{-1}) for several $\text{MCl}_4 \cdot 2\text{L}$ adducts in CH_2Br_2 ^a

	$\nu_1^{cis}(A_1)$	$\nu_2^{cis}(A_1)$	$\nu_1^{trans}(A_{1g})$
$\text{ZrCl}_4 \cdot 2\text{Me}_2\text{O}$ ^b	354(100)	308(38)	
$\text{ZrCl}_4 \cdot 2\text{Me}_2\text{S}$	356(100)	319(78)	
$\text{ZrCl}_4 \cdot 2\text{Me}_2\text{Se}$	354(100)	313(88)	
$\text{ZrCl}_4 \cdot 2(\text{MeO})_3\text{PO}$	332(100)	292(27)	312(59)
$\text{HfCl}_4 \cdot 2\text{Me}_2\text{O}$ ^b	345(100)	304(11)	
$\text{HfCl}_4 \cdot 2\text{Me}_2\text{S}$	347(100)	312(16)	
$\text{HfCl}_4 \cdot 2\text{Me}_2\text{Se}$	344(100)	310(22)	
$\text{HfCl}_4 \cdot 2(\text{MeO})_3\text{PO}$	339(15)	^c	319(100)

^aThe values in parentheses are the relative intensities of the polarized Raman bands. ^bRecorded in $\text{CH}_2\text{Br}_2 \cdot \text{CH}_3\text{NO}_2$ 1:3. ^cToo weak to be observed.

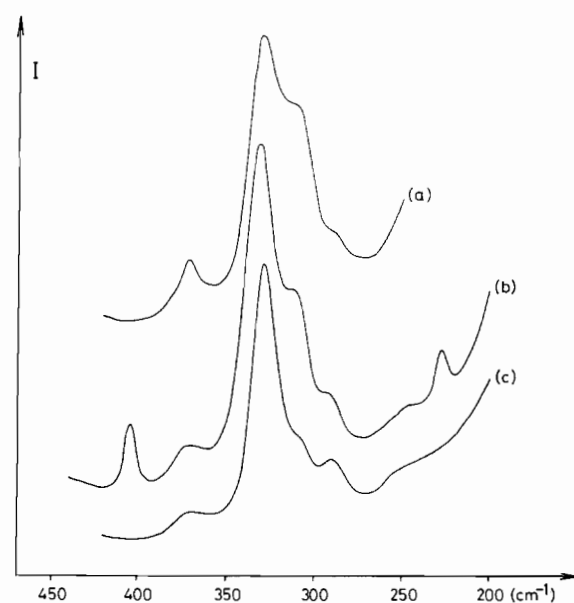


Fig. 1. Raman spectra of a $[\text{ZrCl}_4]:[(\text{MeO})_3\text{PO}] = 1:4$ mixture in (a) CHBr_3 , (b) CH_2Br_2 and (c) CH_3NO_2 .

thus it should be favoured over the *trans* isomer in more polar solvents. Therefore we recorded the vibrational spectrum of $\text{ZrCl}_4 \cdot 2(\text{MeO})_3\text{PO}$ in three solvents of increasing polarity: CHBr_3 ($\epsilon = 4.4$), CH_2Br_2 ($\epsilon = 7.4$) and CH_3NO_2 ($\epsilon = 35.9$) (the $\text{HfCl}_4 \cdot 2(\text{MeO})_3\text{PO}$ adduct decomposed in CH_3NO_2). The series of spectra are shown in Fig. 1 and it can clearly be seen that the band at 312 cm^{-1} in CH_2Br_2 increases in intensity in the less polar CHBr_3 and decreases in intensity in the more polar CH_3NO_2 . The relative intensities of the bands at 292 and 332 cm^{-1} remain constant. This indicates that the band at 312 cm^{-1} is due to the $\nu_1(A_{1g})$ mode of the *trans* isomer as its formation is hampered in more polar solvents.

NMR Spectroscopy: Structure

The solutions of $MCl_4 \cdot 2L$ ($M = Zr, Hf$) adducts used in the NMR study contained an excess of free ligand. If the chemical exchange is slow on the NMR time scale, separate signals are expected for the free ligand and for the coordinated ligand in the *cis* and *trans* isomers, if both are present.

The 1H NMR spectra of a variety of $MCl_4 \cdot 2L$ adducts with dialkylchalcogens as Lewis bases were recorded at low temperatures to try to block the chemical exchange between the free and the coordinated ligand L (see Table 2). In all cases, only the

TABLE 2. 1H NMR chemical shifts in ppm for several $MCl_4 \cdot 2L$ adducts (δ), coalesced signals (δ_{coal}), and free ligands (δ_{free}), in CH_2Cl_2 ^a

	δ	δ_{coal}	δ_{free}	T (K)
$ZrCl_4 \cdot 2Me_2O$	4.08		3.33	202
$ZrCl_4 \cdot 2Me_2S$ ^b		2.49	2.13	134
$ZrCl_4 \cdot 2Me_2Se$		2.26	2.01	179
$ZrCl_4 \cdot 2Et_2S$		2.80 ^c	2.60	183
$ZrCl_4 \cdot 2iPr_2S$		1.26 ^d	1.22	183
$ZrCl_4 \cdot 2tBu_2S$		1.43	1.28	183
$HfCl_4 \cdot 2Me_2S$		2.36	2.13	178
$HfCl_4 \cdot 2Me_2Se$		2.26	2.01	180

^a $[M]_T = 0.050$ m and $[L]_T = 0.200$ m (except for $ZrCl_4 \cdot 2Me_2O$: 0.100 and 0.300 m respectively). ^bIn $CFCl_3$: CD_2Cl_2 1:1. ^cMethylene shift, with $^3J(^1H-^1H) = 7.0$ Hz. ^dMethyl shift, with $^3J(^1H-^1H) = 4.3$ Hz.

coalesced signal could be seen, even at the lowest temperatures attainable without freezing, except for the $ZrCl_4/Me_2O$ solutions, for which two signals were observed at 4.08 and 3.33 ppm. By changing the metal–ligand ratio, the relative populations of the free and bound sites could be varied and the signals were thus assigned to *cis*- $ZrCl_4 \cdot 2Me_2O$ (4.08 ppm) and free Me_2O (3.33 ppm). The high frequency shift due to ligand coordination indicates a reduction in nuclear shielding due to electron donation by the Lewis base. The stoichiometry of *cis*- $ZrCl_4 \cdot 2Me_2O$ was 1:1.99 and was determined by integration of the free and coordinated signals. Proof that the adducts with all other dialkylchalcogen do indeed exist, and that the observed signal is indeed the result of rapid exchange, is provided by comparing the frequency of the observed signal with that of the free ligand. The observed signal is always at a higher frequency than the free ligand, indicating complexation by the Lewis base. In an unsuccessful attempt to slow down the chemical exchange, the 1H NMR spectrum of $ZrCl_4 \cdot 2Me_2S$ was taken in a 1:1 mixture of $CFCl_3$: CH_2Cl_2 at very low temperature (134 K). Complexation with bulky ligands (Et_2S , iPr_2S and tBu_2S) was also tried, but only the coalesced signal was observed in all cases.

1H NMR spectra of $MCl_4 \cdot 2L$ were recorded for two series of phosphoryl ligands: trimethylphosphate ($(MeO)_3PO$), hexamethylphosphoric acid triamide ($(Me_2N)_3PO$) and their mono- and dichloride derivatives. Tables 3 and 4 contain the 1H NMR results for $Zr(IV)$ and $Hf(IV)$ respectively. A typical example,

TABLE 3. 1H NMR chemical shifts (δ ^a), chemical shift differences ($\Delta\delta$ ^b), coupling constants, stoichiometries and isomerization constants^c for $ZrCl_4 \cdot 2L$ adducts with phosphoryl ligands in $CHCl_3$

Ligand (L)	$(MeO)_3PO$	$Cl(MeO)_2PO$	$Cl_2(MeO)PO$	$(Me_2N)_3PO$	$Cl(Me_2N)_2PO$	$Cl_2(Me_2N)PO$
<i>trans</i> - $ZrCl_4 \cdot 2L$						
$\delta \pm 0.01$ (ppm)	4.17	4.33		2.84	2.98	
$\Delta\delta \pm 0.01$ (ppm)	0.39	0.35		0.18	0.25	
$^3J(^1H-^{31}P)$ (Hz) ^d	11.8	14.4		10.2	12.6	
<i>cis</i> - $ZrCl_4 \cdot 2L$						
$\delta \pm 0.01$ (ppm)	4.08	4.26	4.37		2.93	3.10
$\Delta\delta \pm 0.01$ (ppm)	0.30	0.28	0.27		0.20	0.18
$^3J(^1H-^{31}P)$ (Hz) ^d	11.7	14.4	17.2		11.4	16.5
Stoichiometry Zr:L	1:1.98	1:1.94	1:1.70	1:1.98	1:2.02	1:1.97
K_{iso} ($CHCl_3$)	2.04	0.03	0.00 ^e	∞	1.08	0.00
K_{iso} (CH_2Cl_2)	0.69	0.00	0.00 ^e	>50	0.58	0.00
T (K)	217	208	205	278	232	219
$[Zr]_T$ (mol kg ⁻¹)	0.100	0.100	0.025	0.025	0.050	0.050
$[L]_T$ (mol kg ⁻¹)	0.408	0.309	0.117	0.101	0.147	0.214

^aInternal reference was TMS. ^b $\Delta\delta = \delta(ZrCl_4 \cdot 2L) - \delta(L)$. ^c $K_{\text{iso}} = [trans-ZrCl_4 \cdot 2L] / [cis-ZrCl_4 \cdot 2L]$. ^dThe free ligand coupling constants (Hz) are: 11.0 for $(MeO)_3PO$, 14.0 for $Cl(MeO)_2PO$, 17.4 for $Cl_2(MeO)PO$, 9.3 for $(Me_2N)_3PO$, 13.0 for $Cl(Me_2N)_2PO$ and 15.8 for $Cl_2(Me_2N)PO$. ^eIn addition to the *cis* complex, a second species is formed, with $\delta = 4.34$ ppm, $\Delta\delta$ 0.25 ppm and $^3J(^1H-^{31}P) = 17.3$ Hz.

TABLE 4. ^1H NMR chemical shifts (δ^a), chemical shift differences ($\Delta\delta^b$), coupling constants, stoichiometries and isomerization constants^c for $\text{HfCl}_4 \cdot 2\text{L}$ adducts with phosphoryl ligands in CHCl_3

Ligand (L)	(MeO) $_3$ PO	Cl(MeO) $_2$ PO	Cl $_2$ (MeO)PO	(Me $_2$ N) $_3$ PO	Cl(Me $_2$ N) $_2$ PO	Cl $_2$ (Me $_2$ N)PO
<i>trans</i> -HfCl $_4 \cdot 2\text{L}$						
$\delta \pm 0.01$ (ppm)	4.19	4.32		2.83	2.96	3.13
$\Delta\delta \pm 0.01$ (ppm)	0.36	0.35		0.19	0.20	0.21
$^3J(^1\text{H}-^{31}\text{P})$ (Hz) ^d	11.8	14.5		10.0	13.8	16.5
<i>cis</i> -HfCl $_4 \cdot 2\text{L}$						
$\delta \pm 0.01$ (ppm)	4.11	4.25	4.39		2.93	3.10
$\Delta\delta \pm 0.01$ (ppm)	0.29	0.29	0.29		0.17	0.18
$^3J(^1\text{H}-^{31}\text{P})$ (Hz) ^d	11.8	14.5	18.3		13.8	16.5
Stoichiometry Hf:L	1:2.01	1:2.22	1:1.66	1:2.06	1:2.00	1:1.94
K_{iso} (CHCl_3)	3.20	0.40	0.00 ^e	∞	2.00	0.205
K_{iso} (CH_2Cl_2)	1.28	0.18	0.00 ^e	∞	0.60	0.00
T (K)	227	217	215	293	215	223
$[\text{Hf}]_{\text{T}}$ (mol kg $^{-1}$)	0.025	0.025	0.010	0.025	0.025	0.025
$[\text{L}]_{\text{T}}$ (mol kg $^{-1}$)	0.097	0.090	0.028	0.097	0.100	0.101

^aInternal reference was TMS. ^b $\Delta\delta = \delta(\text{HfCl}_4 \cdot 2\text{L}) - \delta(\text{L})$. ^c $K_{\text{iso}} = [\textit{trans}\text{-HfCl}_4 \cdot 2\text{L}]/[\textit{cis}\text{-HfCl}_4 \cdot 2\text{L}]$. ^dThe free ligand coupling constants (Hz) are: 11.0 for (MeO) $_3$ PO, 14.0 for Cl(MeO) $_2$ PO, 17.5 for Cl $_2$ (MeO)PO, 9.3 for (Me $_2$ N) $_3$ PO, 13.2 for Cl(Me $_2$ N) $_2$ PO and 15.8 for Cl $_2$ (Me $_2$ N)PO. ^eIn addition to the *cis* complex, a second species is formed, with $\delta = 4.37$ ppm, $\Delta\delta = 0.27$ ppm and $^3J(^1\text{H}-^{31}\text{P}) = 18.3$ Hz.

the spectrum of $\text{ZrCl}_4 \cdot 2(\text{MeO})_3\text{PO}$ in CHCl_3 at 217 K, Fig. 2(c), contains 3 doublets, each doublet due to $^3J(^1\text{H}-^{31}\text{P})$ splitting. The doublet centred at 3.78 ppm is due to the free (MeO) $_3$ PO and the other two, at 4.08 and 4.17 ppm, to coordinated (MeO) $_3$ PO. As in the case of the vibrational spectra, the coordinated signals were assigned by recording the ^1H NMR spectra in two other solvents of increasing polarity: CH_2Cl_2 , Fig. 2(b), and $\text{CH}_2\text{Cl}_2:\text{CD}_3\text{NO}_2$ 1:1, Fig. 2(a). Thus the doublet centred at 4.08 ppm is due to *cis*- $\text{ZrCl}_4 \cdot 2(\text{MeO})_3\text{PO}$ and that at 4.17 ppm to *trans*- $\text{ZrCl}_4 \cdot 2(\text{MeO})_3\text{PO}$. By analogy, the spectra of the other phosphoryl adducts were assigned to *cis* and *trans* isomers. It is interesting to note that the relative shift of the *trans* signals with respect to the *cis* signals in $\text{ZrCl}_4 \cdot 2(\text{MeO})_3\text{PO}$ is the same as was observed in solutions of $\text{SnCl}_4 \cdot 2(\text{MeO})_3\text{PO}$ [8] and $\text{TiCl}_4 \cdot 2(\text{MeO})_3\text{PO}$ [12]. The stoichiometry of each adduct was 1:2 in all cases except for those adducts formed with Cl $_2$ (MeO)PO, where there was formation of a secondary product (see below).

Both *cis* and *trans* isomers were observed for ZrCl_4 and HfCl_4 adducts with (MeO) $_3$ PO, Cl(MeO) $_2$ PO, Cl(Me $_2$ N) $_2$ PO and for $\text{HfCl}_4 \cdot 2\text{Cl}_2(\text{Me}_2\text{N})\text{PO}$. With (Me $_2$ N) $_3$ PO, in CHCl_3 only the *trans* isomer exists, but in the more polar CH_2Cl_2 three weak supplementary doublets appear in the spectrum of the ZrCl_4 adduct, one of which can be assigned to the *cis* adduct. On the basis of similar findings for $\text{TiCl}_4 \cdot 2(\text{Me}_2\text{N})_3\text{PO}$ and $\text{TiBr}_4 \cdot 2(\text{Me}_2\text{N})_3\text{PO}$ in CH_2Cl_2 [12] and because of the ability of (Me $_2$ N) $_3$ PO to compete

with Cl^- for coordination sites [18], the other two extra doublets were interpreted as evidence for the formation of the ionic complex $[\text{ZrCl}_3 \cdot 3(\text{Me}_2\text{N})_3\text{PO}]^+$. This complex has the structure proposed in Fig. 3. The presence of two inequivalent (Me $_2$ N) $_3$ PO types, α and β , explain the presence of two doublets. *trans*- $\text{HfCl}_4 \cdot 2(\text{Me}_2\text{N})_3\text{PO}$ was the only species observed in either CHCl_3 or CH_2Cl_2 .

Only the *cis* form of $\text{ZrCl}_4 \cdot 2\text{Cl}_2(\text{Me}_2\text{N})\text{PO}$ and $\text{MCl}_4 \cdot 2\text{Cl}_2(\text{MeO})\text{PO}$ (M = Zr, Hf) were observed. When $\text{ZrCl}_4(\text{HfCl}_4)$ are reacted with Cl $_2$ (MeO)PO in CHCl_3 , a second species is formed in addition to the *cis* adduct. In the ^1H NMR spectrum, a doublet centred at 4.34(4.37) ppm, with a splitting of 17.3-(18.3) Hz and a singlet at 3.05 ppm were observed as well as the two doublets for the *cis* and free ligands. The singlet was attributed to CH_3Cl , and the doublet could arise from the species $\text{MCl}_3(\text{O}_2\text{PCL}_2) \cdot \text{Cl}_2(\text{MeO})\text{PO}$. A similar reaction is observed for TiBr_4 in CHBr_3 , where CH_3Br is formed, indicating that the halogen in the latter compound is provided by the metal tetrahalide. Support for the suggested structure of the second product is given by the observation of two types of phosphorus for this species in the $^{31}\text{P}\{^1\text{H}\}$ NMR spectrum (Table 5). For ZrCl_4 there is 55% of the second species, and for HfCl_4 there is 70%.

NMR Spectroscopy: Stability

The isomerization constants, $K_{\text{iso}} = [\textit{trans}\text{-MCl}_4 \cdot 2\text{L}]/[\textit{cis}\text{-MCl}_4 \cdot 2\text{L}]$, (Tables 3 and 4), decrease on

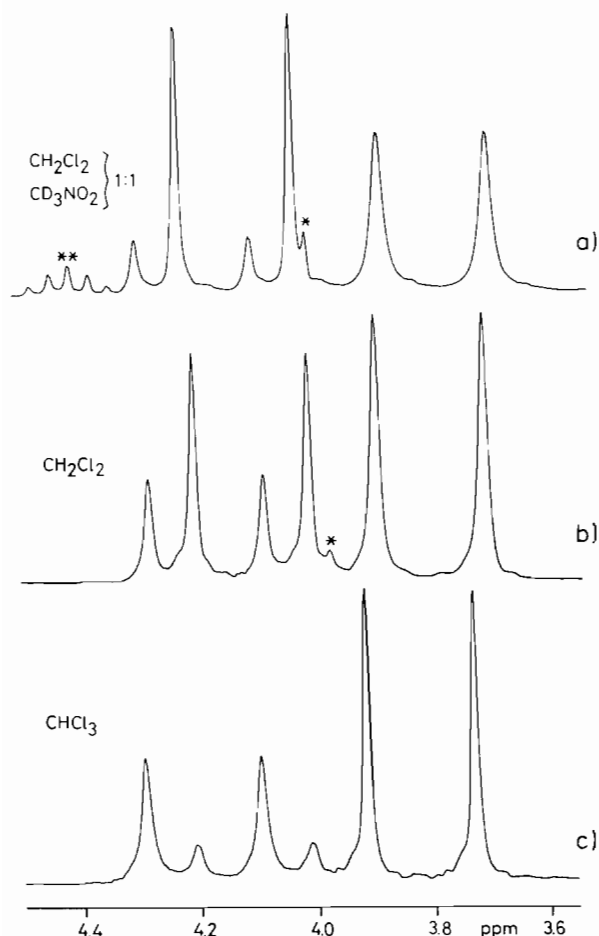


Fig. 2. ^1H NMR spectra (60 MHz) at 213 K of *cis*- and *trans*- $\text{ZrCl}_4 \cdot 2(\text{MeO})_3\text{PO}$ in the presence of excess $(\text{MeO})_3\text{PO}$ in (a) $\text{CH}_2\text{Cl}_2:\text{CD}_3\text{NO}_2$ 1:1, (b) CH_2Cl_2 and (c) CHCl_3 . $[\text{ZrCl}_4 \cdot 2(\text{MeO})_3\text{PO}] = 0.025$ m, $[\text{Free } (\text{MeO})_3\text{PO}] = 0.05$ m. ^{13}C satellite of CH_2Cl_2 , ** CHD_2NO_2 solvent peaks.

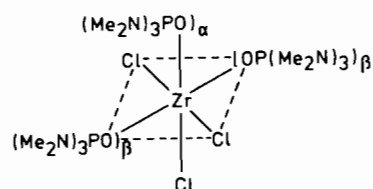


Fig. 3. Proposed structure of the cationic species $[\text{ZrCl}_3 \cdot 3(\text{Me}_2\text{N})_3\text{PO}]^+$.

going from CHCl_3 to the more polar solvent CH_2Cl_2 . For $\text{ZrCl}_4 \cdot 2(\text{MeO})_3\text{PO}$ in CHCl_3 , K_{iso} is practically invariant with temperature. The variation with pressure (up to *c.* 200 MPa) of K_{iso} has been measured at 244.15 K in CHCl_3 by ^1H NMR (11 measurements, $K_{\text{iso}}(P = 0.1 \text{ MPa}) = 2.17$ and $K_{\text{iso}}(P = 198.5 \text{ MPa}) = 1.48$; experimental, see ref. 19) leading to a reaction volume, $\Delta V_{\text{iso}}^\circ = +3.8 \pm 0.4 \text{ cm}^3 \text{ mol}^{-1}$.

In order to determine the relative stability constants, $K_{\text{a,b}}^1$, of a series of *i*- $\text{MCl}_4 \cdot 2\text{L}$ (*i* = *cis*, *trans*)

TABLE 5. $^31\text{P}\{^1\text{H}\}$ NMR chemical shifts (δ^{a}), and chemical shift differences ($\Delta\delta^{\text{b}}$) for $\text{ZrCl}_4 \cdot 2\text{L}$ and $\text{HfCl}_4 \cdot 2\text{L}$ adducts with phosphoryl ligands in CHCl_3

Ligand (L)	$\text{ZrCl}_4 \cdot 2\text{L}$		$\text{HfCl}_4 \cdot 2\text{L}$		$\text{Cl}(\text{MeO})_2\text{PO}$	$\text{Cl}_2(\text{MeO})\text{PO}^{\text{d}}$	Cl_3PO
	$(\text{MeO})_3\text{PO}$	$(\text{MeO})_2\text{PO}$	$(\text{MeO})_3\text{PO}$	$(\text{MeO})_2\text{PO}$			
<i>trans</i> - $\text{MCl}_4 \cdot 2\text{L}$							
$\delta \pm 0.01$ (ppm)	-4.2		-3.9		4.3	23.2	31.2
$\Delta\delta \pm 0.01$ (ppm)	-6.4		-6.0		1.5	17.1	25.0
<i>cis</i> - $\text{MCl}_4 \cdot 2\text{L}$							
$\delta \pm 0.01$ (ppm)		-3.6		-3.1	3.9	23.2	31.2
$\Delta\delta \pm 0.01$ (ppm)		-5.8		-5.2	1.0	17.1	25.0
Stoichiometry M:L		1:1.99		1:1.98	1:2.10	1:2.04	1:1.98
<i>T</i> (K)		251		243	225	225	225
$[\text{M}]_{\text{T}}$ (mol kg^{-1})		0.10		0.05	0.05	0.05	0.05
$[\text{L}]_{\text{T}}$ (mol kg^{-1})		0.30		0.20	0.20	0.20	0.20

^aExternal reference was 62.5% H_3PO_4 . ^b $\Delta\delta = \delta(\text{MCl}_4 \cdot 2\text{L}) - \delta(\text{L})$. ^cFormation of a second product, $\text{ZrCl}_4(\text{O}_2\text{P}_\alpha\text{Cl}_2) \cdot \text{Cl}_2(\text{MeO})\text{PO}_\beta\text{O}$, with chemical shifts $\delta_\alpha = 6.2$ ppm and $\delta_\beta = 21.3$ ppm. ^dFormation of a second product, $\text{HfCl}_4(\text{O}_2\text{P}_\alpha\text{Cl}_2) \cdot \text{Cl}_2(\text{MeO})\text{PO}_\beta\text{O}$, with chemical shifts $\delta_\alpha = 8.7$ ppm and $\delta_\beta = 22.2$ ppm.

TABLE 6. Estimated relative stability constants for *cis*- and *trans*-ZrCl₄·2L and HfCl₄·2L adducts^a with phosphoryl ligands in CHCl₃ at 213 K

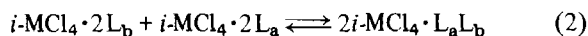
L _a	L _b	K _{a,b} ^t	K _{a,b} ^c	K _{a,b} ^t /K _{a,b} ^c	K _{iso} ^a /K _{iso} ^b
ZrCl ₄ ·2L					
(Me ₂ N) ₃ PO	Cl(Me ₂ N) ₂ PO	≥ 10 ⁵			
Cl(Me ₂ N) ₂ PO	(MeO) ₃ PO	14	23	0.61	0.53 ^b
(MeO) ₃ PO	Cl(MeO) ₂ PO		≥ 10 ⁴		
Cl(MeO) ₂ PO	Cl ₂ (Me ₂ N)PO		270		
HfCl ₄ ·2L					
(Me ₂ N) ₃ PO	Cl(Me ₂ N) ₂ PO	≥ 10 ⁵			
Cl(Me ₂ N) ₂ PO	(MeO) ₃ PO	9	23	0.39	0.62 ^c
(MeO) ₃ PO	Cl(MeO) ₂ PO		≥ 10 ⁵		
Cl(MeO) ₂ PO	Cl ₂ (Me ₂ N)PO	600	278	2.16	1.95 ^c

^a [M]_T = 0.025 m, [L_a]_T + [L_b]_T = 0.100m.^b From Table 3.^c From Table 4.

for a given metal halide, the equilibrium (1) has been considered for a few pairs of Lewis bases



The stability constants were obtained by integration of the ¹H NMR signals of the species in equilibrium as described by Ruzicka and Merbach [8]. It was assumed that the mixed ligand species, *i*-MCl₄·2L_aL_b, were formed (eqn. (2)) in statistical proportions (equilibrium constant = 4).



In this case the relative stability constants are related to the isomerization constant, K_{iso}, by eqn. (3)

$$K_{a,b}^t/K_{a,b}^c = K_{iso}^a/K_{iso}^b \quad (3)$$

The results are given in Table 6 and lead to the following stability sequence: (Me₂N)₃PO ≫ Cl(Me₂N)₂PO > (MeO)₃PO ≫ Cl(MeO)₂PO > Cl₂(Me₂N)PO.

Discussion

Structure

Solid adducts of ZrCl₄ and HfCl₄ with organic ligands are well known, and vibrational spectroscopy has been used to characterize a number of solid adducts with ethers, sulphides, nitriles, amines, phosphines, arsines and other organic ligands [20–26]. A vibrational spectroscopy study of ZrX₄·2NMe₃ (X = Cl, Br, I) and HfCl₄·2NMe₃ [27, 28] revealed that these adducts were of *cis* configuration, except that with the softest Lewis acid: *trans*-ZrI₄·2NMe₃. The main theories proposed for expected adduct structure pertain to steric factors [29] and halogen–metal p_π–d_π interactions [29, 30].

The steric approach proposes the preferential formation of the *cis* adduct when the donor atom of

the ligand is smaller than the halogen, because in the *cis* adduct the halogens can distort to give a pseudo-tetrahedral structure, thus decreasing halogen–halogen interaction. Conversely, if the donor atom of the ligand is larger than the halogen, or if the ligand is sterically encumbered, then the ligand–halogen and ligand–ligand interactions predominate and the *trans* isomer will be favoured.

Steric interactions alone are not sufficient to explain the observed structures, and the effect of p_π–d_π backbonding, between the filled p orbital of the halogen and the empty t_{2g} orbitals of the metal, must also be considered [29, 30]. The halogen atom competes for the available M–d_π orbitals with the ligand *trans* to itself, and it can compete more successfully if this *trans* ligand is a weaker π electron donor. The *cis* adduct is thus favoured in this case. If the Lewis base is a better electron donor than the halogen, the *trans* adduct will be favoured, and if the Lewis base is of about the same strength as the halogen, p_π–d_π backbonding effects are unimportant in deciding the stereochemistry of the adduct. Experimentally, it was found that *trans* adducts were favoured when strong Lewis base ligands were used.

The above arguments can be applied to the ZrCl₄ and HfCl₄ dialkylchalcogen adducts studied in this work, where adducts of both metal tetrachlorides exist only in the *cis* configuration. This is as expected for weak π electron donors and is comparable to what was established for TiCl₄·2L adducts [12]. SnCl₄·2L dialkylchalcogen adducts show both *cis* and *trans* isomers [7], but p_π–d_π considerations do not seem to be as important in the formation of the d¹⁰ SnCl₄·2L adducts [30].

The structures of the various ZrCl₄ and HfCl₄ adducts with phosphoryl ligands can also be explained using the above criteria. A *trans* configuration would be favoured for adducts formed with strongly basic ligands [30], and with bulky ligands

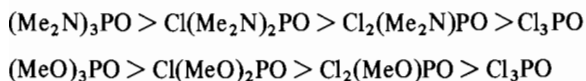
where steric factors would be important. The combination of these effect explains the observed configurations. Only the *trans* isomer is found for $\text{MCl}_4 \cdot 2(\text{Me}_2\text{N})_3\text{PO}$, which has the most basic and bulkiest ligand; both *cis* and *trans* isomers occur for $\text{MCl}_4 \cdot 2\text{Cl}(\text{Me}_2\text{N})_2\text{PO}$, $\text{MCl}_4 \cdot 2(\text{MeO})_3\text{PO}$, $\text{MCl}_4 \cdot 2\text{Cl}(\text{MeO})_2\text{PO}$ and $\text{HfCl}_4 \cdot 2\text{Cl}_2(\text{Me}_2\text{N})\text{PO}$ and only the *cis* isomer is observed for $\text{ZrCl}_4 \cdot 2\text{Cl}_2(\text{Me}_2\text{N})\text{PO}$, $\text{MCl}_4 \cdot 2\text{Cl}_2(\text{MeO})\text{PO}$ and $\text{MCl}_4 \cdot 2\text{Cl}_3\text{PO}$. This last adduct contains the weakest Lewis base and least bulky ligand. Both *cis* and *trans* isomers exist for $\text{HfCl}_4 \cdot 2\text{Cl}_2(\text{Me}_2\text{N})\text{PO}$, but only *cis*- $\text{ZrCl}_4 \cdot 2\text{Cl}_2(\text{Me}_2\text{N})\text{PO}$ is found. Since HfCl_4 is a softer Lewis acid than ZrCl_4 , it considers $\text{Cl}_2(\text{Me}_2\text{N})\text{PO}$ to be a stronger base than would ZrCl_4 and thus a *trans* isomer is a more probable occurrence.

The results of this study can be compared to those obtained for $\text{TiCl}_4 \cdot 2\text{L}$ adducts with the same ligands, where only the *cis* isomer exists, except for those adducts containing Lewis base ligands with good π -donating power ($\text{L} = (\text{MeO})_3\text{PO}$, $(\text{Me}_2\text{N})_3\text{PO}$ and $\text{Cl}(\text{Me}_2\text{N})_2\text{PO}$). The hardness of the Lewis acid decreases on going from TiCl_4 to HfCl_4 , and it would seem that the tendency to form a *trans* isomer increases inversely with the hardness of the acid: $\text{TiCl}_4 > \text{ZrCl}_4 > \text{HfCl}_4$.

Stability

In the case of ZrCl_4 and HfCl_4 adducts with dialkylchalcogens, intermolecular Lewis base exchange was too rapid for the determination of a stability series. For the similar *cis*- $\text{TiCl}_4 \cdot 2\text{L}$ [12] and $\text{SnCl}_4 \cdot 2\text{L}$ [7, 8] adducts the stability sequence is $\text{Me}_2\text{Se} \gg \text{Me}_2\text{S} \gg \text{Me}_2\text{O}$.

The phosphoryl ligands chosen for this study form a well defined succession of π -electron donors as the successive replacement of MeO or the stronger electron donor, Me_2N , by the electron acceptor Cl decreases the electron donor strength of the phosphoryl oxygen [30], giving the following sequences



where $(\text{Me}_2\text{N})_3\text{PO}$ is the strongest Lewis base and Cl_3PO the weakest. The stability series observed for $\text{ZrCl}_4 \cdot 2\text{L}$ and $\text{HfCl}_4 \cdot 2\text{L}$ adducts are shown in Table 6: $(\text{Me}_2\text{N})_3\text{PO} \gg \text{Cl}(\text{Me}_2\text{N})_2\text{PO} > (\text{MeO})_3\text{PO} \gg \text{Cl}(\text{MeO})_2\text{PO} > \text{Cl}_2(\text{Me}_2\text{N})\text{PO}$, and are compatible with the above sequences. It was not possible to measure the relative stabilities of the Zr adducts with respect to the Hf adducts, using competitive equilibria for a given Lewis base, because of solubility problems. ZrCl_4 and HfCl_4 are insoluble in the solvents used; only the adduct dissolves and thus excess ligand must be used. The relative stability sequence found for $\text{MCl}_4 \cdot 2\text{L}$ ($\text{M} = \text{Zr}, \text{Hf}$) is the same as those found for

$\text{TiCl}_4 \cdot 2\text{L}$ [12], $\text{SnCl}_4 \cdot 2\text{L}$ [7] and $\text{MX}_5 \cdot \text{L}$ ($\text{M} = \text{Nb}, \text{Ta}$) [2, 3] and the arguments of steric and electronic effects provide adequate explanations in all cases.

For those adducts showing both *cis* and *trans* isomers, the relative stability constants are theoretically connected to the isomerization constants K_{iso} by eqn. (3). These ratios, where applicable, are given in Table 6. The agreement is reasonable and any differences can be explained by experimental error and the fact that the formation constant for mixed ligand species, eqn. (2), may not be equal to 4.

The effect of pressure on the *cis*-*trans* isomerization equilibrium for $\text{ZrCl}_4 \cdot 2(\text{MeO})_3\text{PO}$ in CHCl_3 at 244.15 K yielded $\Delta V_{\text{iso}}^\circ = +3.8 \pm 0.4 \text{ cm}^3 \text{ mol}^{-1}$, which means that the *cis* isomer is favoured over the *trans* at high pressure. This is as expected because electrostriction on the *cis* isomer will be greater due to its non-zero dipole moment. A similar result was obtained [11] for Me_2S exchange on $\text{SnCl}_4 \cdot 2\text{Me}_2\text{S}$ ($\Delta V_{\text{iso}}^\circ = +3.2 \pm 0.4 \text{ cm}^3 \text{ mol}^{-1}$). For $\text{TiCl}_4 \cdot 2(\text{MeO})_3\text{PO}$, $\Delta V_{\text{iso}}^\circ$ is close to zero ($-1.3 \pm 0.8 \text{ cm}^3 \text{ mol}^{-1}$) [12], but perhaps other factors come into play with the Ti^{4+} ion.

In conclusion, ZrCl_4 and HfCl_4 adducts with neutral Lewis base ligands display a variety of configurations in solution, ranging from only *cis*, through *cis*-*trans* equilibria, to only *trans*. The configurations and relative stabilities of the adducts can be explained using steric and electronic arguments. The relative stability sequence found for adducts with phosphoryl ligands is the same as that already observed for $\text{TiCl}_4 \cdot 2\text{L}$, $\text{SnCl}_4 \cdot 2\text{L}$, $\text{NbCl}_5 \cdot \text{L}$ and $\text{TaCl}_5 \cdot \text{L}$.

Acknowledgements

We thank Dr E. Turin for the vibrational spectra and the Swiss National Science Foundation for financial support through Grant No. 2.672-0.87.

References

- 1 R. Good and A. E. Merbach, *Inorg. Chem.*, **14** (1975) 1030.
- 2 R. Good and A. E. Merbach, *Helv. Chim. Acta*, **57** (1974) 1192.
- 3 C. P. Favez, H. Rollier and A. E. Merbach, *Helv. Chim. Acta*, **59** (1976) 2383.
- 4 H. Vanni and A. E. Merbach, *Inorg. Chem.*, **18** (1979) 2758.
- 5 J.-E. Kessler, C. T. G. Knight and A. E. Merbach, *Inorg. Chim. Acta*, **115** (1986) 75.
- 6 J.-E. Kessler, C. T. G. Knight and A. E. Merbach, *Inorg. Chim. Acta*, **115** (1986) 85.
- 7 S. J. Ruzicka, C. M. P. Favez and A. E. Merbach, *Inorg. Chim. Acta*, **23** (1977) 239.
- 8 S. J. Ruzicka and A. E. Merbach, *Inorg. Chim. Acta*, **20** (1976) 221.
- 9 S. J. Ruzicka and A. E. Merbach, *Inorg. Chim. Acta*, **22** (1977) 191.

- 10 C. T. G. Knight and A. E. Merbach, *J. Am. Chem. Soc.*, **106** (1984) 804.
- 11 C. T. G. Knight and A. E. Merbach, *Inorg. Chem.*, **24** (1985) 576.
- 12 E. Turin, R. M. Neilson and A. E. Merbach, *Inorg. Chim. Acta*, **134** (1987) 67.
- 13 E. Turin, R. M. Neilson and A. E. Merbach, *Inorg. Chim. Acta*, **134** (1987) 79.
- 14 C. Ammann, P. Meier and A. E. Merbach, *J. Magn. Reson.*, **46** (1982) 319.
- 15 U. Frey, L. Helm and A. E. Merbach, *High Pressure Res.*, in press.
- 16 F. K. Meyer and A. E. Merbach, *J. Phys. E.*, **12** (1979) 185.
- 17 I. R. Beattie, M. Webster and G. W. Chantry, *J. Chem. Soc.* (1964) 6172.
- 18 A. I. Kuzmin and S. I. Kuznetsov, *Soviet. J. Coord. Chem. (Engl. Transl.)*, **8** (1983) 81.
- 19 M. Turin-Rossier, D. Hugi-Cleary, U. Frey and A. E. Merbach, *Inorg. Chem.*, submitted for publication.
- 20 G. W. A. Fowles and R. A. Walton, *J. Less-Common Met.*, **5** (1963) 510.
- 21 I. R. Beattie and M. Webster, *J. Chem. Soc.* (1964) 3507.
- 22 G. W. A. Fowles and R. A. Walton, *J. Chem. Soc.* (1964) 4330.
- 23 T. C. Ray and A. D. Westland, *Inorg. Chem.*, **4** (1965) 1501.
- 24 E. C. Aleyea and E. G. Torrible, *Can. J. Chem.*, **43** (1965) 3468.
- 25 S. C. Jain, *J. Inorg. Nucl. Chem.*, **35** (1973) 505.
- 26 L. M. Larsen and T. E. Henzler, *Inorg. Chem.*, **13** (1974) 581.
- 27 J. Hugues and G. R. Willey, *Inorg. Chim. Acta*, **20** (1976) 137.
- 28 G. R. Willey, *Inorg. Chim. Acta*, **21** (1977) L12.
- 29 I. R. Beattie, *Q. Rev.*, **17** (1963) 382.
- 30 D. S. Dyer and R. O. Ragsdale, *Inorg. Chem.*, **8** (1969) 1116.